 doi:10.20944/preprints202105.0738.v1

Research on parameters of wire-filling laser welding and quenching process for joints microstructure and mechanical property of BR1500HS steel

Lianpu Zhou[1,2], Chundong Zhu[1,2,3,] *, Rongfei Ma[1] and Zihao Wei[1,3]

[1] School of Materials Science and Engineering, Wuhan University of Technology, Wuhan, 43007, China; thz918618@whut.edu.cn (L.Z.); zcdzcd6252@sina.com (C.Z.); mrf278305@163.com (R.M.); weizihao@whut.edu.cn (Z.W.)
[2] Hubei Center for Quality Inspection of Special Purpose Vehicles, SuiZhou, 441300, China;
[3] Suizhou-WUT Industry Research Institute, SuiZhou, 441300, China;
* Correspondence: zcdzcd6252@sina.com;

Abstract: With the aim to investigate the effect of parameter and quenching process on the joint of hot stamping steel by laser welding, the BR1500HS boron steel was welded by filling-wire laser welding with ER70-G welding wire under different parameters. The welded specimens were heated to 900℃ and held for 5min before water quenching. The universal material test machine, Optical microscope, Vickers hardness tester, scanning electron microscope and electron backscatter diffraction (EBSD) were used to characterize. The results showed that the macroscopic morphology of fusion zone (FZ) becomes from funnelform to hyperbolic curve shape when heat input increases and from hyperbolic curve shape to funnelform when wire-feed speed increases. The strength after quenching is more than 1557Mpa at heat input of 1040J/cm, wire feeding speed of 1.6m/min~1.8m/min and welding speed of 1.5m/min. EBSD test showed that the FZ and fine grain zone (FGZ) have more retained austenite (RA) than coarse grain zone (CGZ) before quenching and RA in FZ and heat affect zone (HAZ) decreased and distributed uniformed after quenching. The grain diameter in FZ distribute unevenly, with the maximum grain diameter larger than 40μm before quenching. After quenching, the grain diameter of FZ, HAZ and BM is more even and coarse grains in the FZ was refined. Before quenching, the microhardness of FZ and HAZ is of 450HV~500HV at different heat input and wire-feed speed and all region of joint keeps at 450HV~550HV after quenching. Most dimple and little river pattern in the joint fracture morphology before quenching indicates a well plasticity and most cleavage facet is observed after quenching due to the joint combine with martensite.

Keywords: Wire-filling laser welding; Quenching; Process parameters; Grain diameter; Retained austenite

1. Introduction

In the tendency of current automotive lightweight, automotive parts are applying more and more high strength steel to reduce weight [1]. However, automobile parts inevitably need to be connected by welding technology and the heat affected zone is easy to soften due to the effect of thermal circulation in the welding process for high strength steel, which dramatically decreases the strength of the joint. In order to meet the welding demand of high strength steel, reduce the defects in the welding process, laser welding technology has been applied more and more widely recently [2]. Laser welding has many advantages such as high heat input, concentrated energy, fast cooling rate, narrow heat affected zone and excellent joint property, etc, applying more frequently for the connection of high strength steel [3-4]. According to whether filling wire material or not, laser welding can be divided into autogenously laser welding and wire-filling laser welding [5]. For autogenously laser welding, the assembly precision of workpiece is very high and

Preprints (www.preprints.org) | NOT PEER-REVIEWED | Posted: 31 May 2021 doi:10.20944/preprints202105.0738.v1

no gap is allowed in the joint. Otherwise, the slim laser beam will pass through the gap of joint so that the base material can't be melted fully to form a qualified joint. For wire-filling laser welding, laser beam fuses the wire material to fill the gap to obtain the welding joint [6]. Therefore, wire-filling laser welding can allow a small gap in the join, which can solve the problem that the high assembly precision of joint of autogenously laser welding [7]. Moreover, filling materials can also adjust the chemical composition for welding joint, realize metallurgical treatment and obtain better mechanical properties [8-10]. So, it is meaningful to carry out an experiment to investigate the process parameters, microstructure and mechanical properties of wire-filling laser welding for high strength steel.

Many researchers have carried a lot of experiment and investigations of wire-filling laser welding for high strength steel. Himani Siva Prasad et al. [3] investigated the stability of laser welding with respect to the parameters as gap width, welding speeds and powers. Mei Yang et al. [11] studied the effect of welding speed on 2195 aluminium–lithium (Al–Li) alloy joints welded by laser and metal inert gas (laser-MIG) hybrid welding using Al–Si welding wire. Ho Won Lee et al. [12] investigated the effect of post-welding heat treatment (PWHT) of quenching and tempering (QT) on the microstructure and mechanical properties of welded boron steel joints processed using laser-arc hybrid welding on two commercial filler materials SM80 (Type-I) and ZH120 (Type-II). Muyu Li et al. [13] researched the effects of welding speed and post quenching on the joint microstructure microhardness, and high-temperature tensile properties.

Hot stamping steel is an advanced ultra-high strength steel, which contains a few boron elements, which inhibits the precipitation of ferrite during cooling and make it easier to obtain martensite with very high strength. At present, hot stamping steel has widely used in automobile B pillar, anti-collision beam and other structures [14]. But hot stamping steel possesses a poor welding performance for the tendency of heat affected zone (HAZ) softening phenomenon after quenching process [15-16]. Therefore, it is essential to investigate the welding process before the quenching state of hot stamping steel and the effect of quenching process for the microstructure and mechanical properties of joint. Besides, the welding process of hot stamping steel concentrate more on the autogenously laser welding and less on the wire-feeding laser welding. So, the study of wire-feeding laser welding for hot stamping steel has more space to carry out.

In this paper, hot stamping steel of BR1500HS and ER70-G welding wire were used to investigate wire-filling laser welding under different parameters before specimens quenching. Then, the welded specimens were heated and quenched by water to research the effect of laser welding parameters and quenching process for macro morphology, microstructure, microhardness, tensile strength and fracture morphology of the welding joint.

2. Materials and Methods

Materials

The 3.5mm thickness hot-rolled boron steel BR1500HS was used as the experimental sample material, which was provided by Baosteel (Shanghai, China). The welding wire used for the welding process is ER70-G, with a diameter of 1.2mm and ultimate tensile strength of 690MPa before quenching. The chemical composition of BR1500HS and ER70-G welding wire was shown in **Tab.1**. The ultimate tensile strength of BR1500HS is about 630MPa, elongation of 15% before quenching and strength of 1500-1800MPa, elongation of 6% after quenching treatment. The matrix microstructure before quenching is consists of ferrite and pearlite.

Table 1. The chemical composition of BR1500HS and ER70-G wire

	C	Si	Mn	Cr	Ni	Mo	B	Al	Ti	Cu	V	S	P
BR1500HS	0.23	0.25	1.35	0.19	0.028	0.04	0.003	0.04	0.03	0.016	0.004	0.006	0.015
ER70-G	0.1	0.6	1.6	-	0.7	0.4	-	-	0.2	0.5	-	0.025	0.025

Preprints (www.preprints.org) | NOT PEER-REVIEWED | Posted: 31 May 2021 doi:10.20944/preprints202105.0738.v1

Laser welding and quenching

The equipment used for laser welding was RFL-C4000 fiber laser system (Raycuslaser Co., Ltd. Wuhan, China), with a maximum power of 4KW and the wavelength of 1080±5nm. The welding operation was performed by industrial robot MOTOMAN-GP50 (Yaskawa Electric (China) Co., Ltd. Shanghai, China). The sheet was processed into samples with dimension of 240mm×120mm. The samples were polished by sandpaper to remove the rust and oil before welding. The pure argon was used as the shielding gas, with a flow of 15L/min. The butt joint gap was 0.5mm in the fixture and the welding parameters of laser power, welding speed and wire feeding speed for samples were shown in **Tab.2**. The schematic of wire-filling laser welding and field experiment photo were shown in **Fig.1**. When the welding process finished, samples were processed into tensile test specimens by wire-electrode cutting and the dimension was shown in **Fig. 2**. For quenching process, the temperature was kept at 900℃ and the samples were put into the furnace and hold for 5mm before quenching in water.

Table 2. the parameter of experimental laser welding sample

No.	Laser power (w)	Wire feeding speed (m/min)	Welding speed (m/min)
1#-5#	1800, 2200, 2600, 3000, 3400	1.8	1.5
6#-9#	2600	1.4, 1.6, 2.0, 2.2	1.5

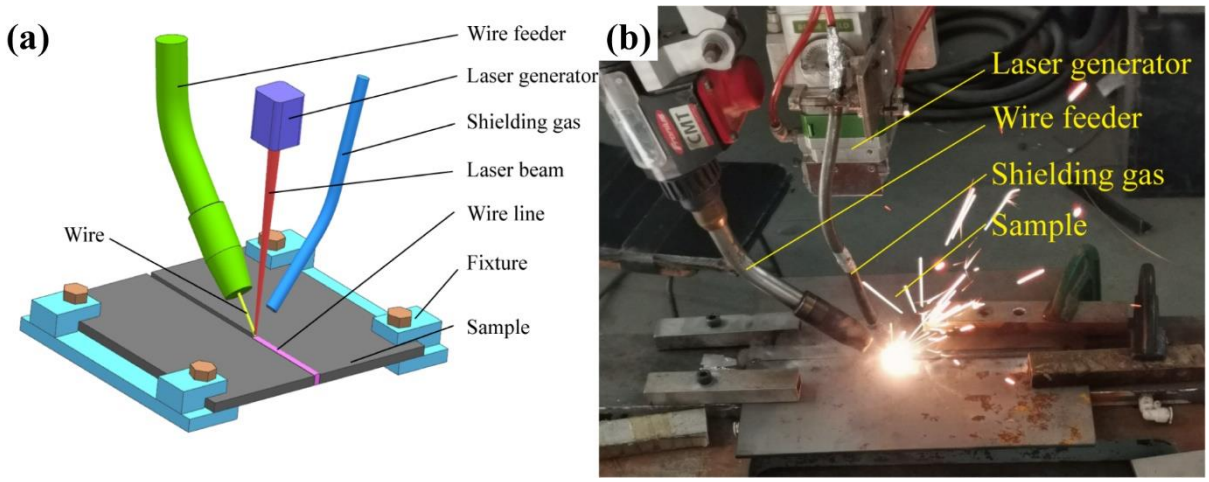

Figure 1. The description of wire-filling laser welding (a) Schematic diagram (b)Field experiment

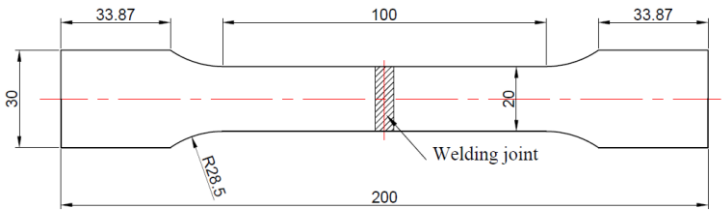

Figure 2. The dimension of tensile sample (Unite: mm)

Characterization

The tensile strength of samples before and after quenching was test on SHT4106 universal material test machine (MTS System, Eden Prairie, USA), with a loading speed of 1mm/min. Metallographic specimens were polished with 240, 400, 800, 1200, 1500 mesh sandpaper and mechanically polished with 1um diamond polishing fluid until the mirror surface. Then, specimens were corroded with 4% nitric acid alcohol for 10-20s and then washed by anhydrous alcohol. The Zeiss Axio Scope A1 (ZEISS, Jena, Germany) Optical microscope (OM) was used to observe the joint macroscopic morphology and

Preprints (www.preprints.org) | NOT PEER-REVIEWED | Posted: 31 May 2021 doi:10.20944/preprints202105.0738.v1

microstructure of heat-affected zone at 50-500 times. The Electron Backscatter Diffraction (EBSD) specimens were burnished with sandpaper, polished with 9um, 3um, 1um diamond polishes and polished with OPS finally. The EBSD test was performed by Quanta FEG 450 scanning electron microscopes (SEM) with EBSD detector (EDAX, LLC. Mahwah, USA) to obtain the grain diameter, grain orientation and fraction of retained austenite of heat-affected zone. The microhardness of the weld joint was tested by HV-1000A (Laizhou Huayin, Laizhou, China) Vickers hardness tester, with a loading force of 500g (4.9N) and the pressure holding time of 10s. As showed in **Fig.3**, the microhardness test position of the joint is in the middle of the joint cross section and interval of 0. 1mm.The fracture morphology of tensile specimens was observed by Hitachi SU8010 (Hitachi, Ltd. Tokyo, Japan) high-resolution field emission scanning electron microscope (SEM) at 1000-5000 times.

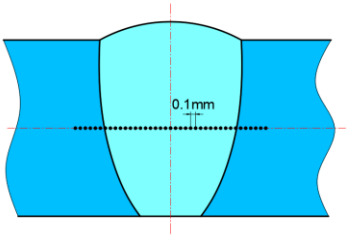

Fig.3 The position of joint microhardness test

3. Results and Discussion

3.1. Tensile test results

The tensile strength and fracture position of samples before and after quenching were showed in **Tab.3.** Before quenching, only strength of sample No.1, 2 and 6 was extremely low, with 372MPa, 514.2MPa, 574MPa respectively, so the fracture position was at the joint due to the strength lower than base material (BM). The strength of all other samples had exceeded the strength of the BM before quenching, with the fracture position of BM. However, the strength of BR1500HS quenched can reach 1800Mpa at maximum, which is difficult for the weld joint to exceed it after quenching. So, it could be seen that all fracture positions of samples quenched are at weld joint.

Table 3. Tensile strength and fracture position of samples before and after quenching

No.	power (w)	Wire feeding speed (m/min)	Welding speed (m/min)	Before quenching		After quenching	
				Tensile strength/MPa	Fracture position	Tensile strength/MPa	Fracture position
1#	1800	1.8	1.5	372	Joint	726	Joint
2#	2200	1.8	1.5	514.2	Joint	981	Joint
3#	2600	1.8	1.5	635	BM	1557	Joint
4#	3000	1.8	1.5	632.8	BM	1653	Joint
5#	3400	1.8	1.5	619	BM	1663	Joint
6#	2600	1.4	1.5	574	Joint	612	Joint
7#	2600	1.6	1.5	627.9	BM	1653	Joint
8#	2600	2.0	1.5	629.3	BM	1309	Joint
9#	2600	2.2	1.5	631	BM	1376	Joint

Macro morphology and strength

The influence of heat input on morphology and strength

Preprints (www.preprints.org) | NOT PEER-REVIEWED | Posted: 31 May 2021 doi:10.20944/preprints202105.0738.v1

For wire-filling laser welding process, the parameters of laser power, welding speed have a great influence on the appearance and properties of the joint. The higher the laser power and the more melting volume of the wire and BM, so the wider the fusion zone (FZ) and heat affected zone (HAZ) [17]. When the welding speed increases, the effect of heat on the weld per unit length is less, reducing the melting volume of the welding wire and BM. Then the temperature of weld is lowered, and the width of the weld and heat affected zone is narrowed [18-19].

When the wire feeding speed of 1.8m/min and welding speed of 1.5m/min, the morphology of the joint under different heat input is shown in **Fig.4**. When the heat input is 720J/cm, it can be observed from the **Fig.4(a)** that a high reinforcement existed in the top surface of the weld, but the lower surface has a root underfill defect, resulting in a gap in the joint due to the low heat input. So, the lower half of the weld is subjected to weak thermal action and the BM can't be melted. Besides the weld cooling fast, molten metal solidified and stacked at the top surface forming an obvious reinforcement before fulfilling the bottom weld. When the heat input is 880J/cm, both the upper and lower surfaces of the base material have been melted and there is no obvious non-penetration defect at this time. However, when the heat input is 720J/cm and 880J/cm, due to the low heat input, the upper surface of the joint is subjected to strong thermal action with forming a wide heat affected zone. And lacking of heat on the middle and lower surfaces, the width of the heat affected zone of the weld becomes narrower. Therefore, the macro morphology of joint at low heat input shows a funnel-shaped. When the heat input increases to more than 1040J/cm, the heat input is enough to penetrate the upper and lower surfaces of the entire weld section, and the width of the heat affected zone above and below the weld is basically the same, showing a hyperbolic curve shape. If the heat input reaches more than 1200J/cm and continues to increase to 1360J/cm, it can be found that the width of the heat-affected zone becomes larger. Moreover, due to the concentration of laser welding heat sources, the upper surface of the weld appears sinking, which seriously affects the weld morphology. Therefore, when the wire feeding speed of 1.8m/min, it is easier to obtain the best macroscopic morphology at heat input of 1040J/cm~1200J/cm.

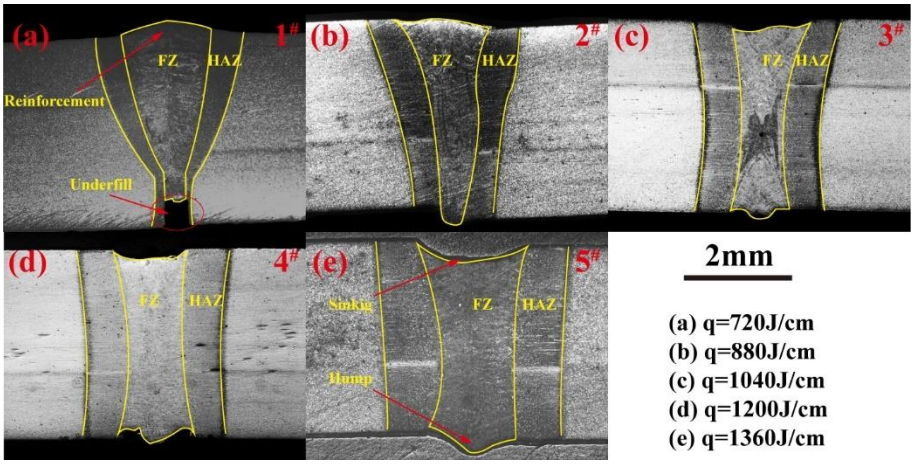

Figure 4. Macro morphology of joint at different heat input

The samples and tensile strength of the joint at different heat input are shown in the **Fig.5**. When the heat input is 720J/cm and 880J/cm, the fracture position on the joint before quenching, and the strength is 372MPa and 514.2MPa respectively. The strength before quenching is seriously unqualified, so the strength after quenching was only 726MPa and 981MPa. The low heat input led to underfill defects reduce the joints strength. When the heat input is 1040J/cm, the strength of the weld has exceeded the strength of the BM before quenching and with a high strength of 1557MPa after quenching. Then when the heat input increases to 1200J/cm and even 1360J/cm, the strength improvement after quenching is not obvious. Therefore, the influence of heat input on the weld strength is obvious at

Preprints (www.preprints.org) | NOT PEER-REVIEWED | Posted: 31 May 2021 doi:10.20944/preprints202105.0738.v1

the initial stage when the heat input was very low, but when the heat input more than 1200J/cm, its influence is not very obvious.

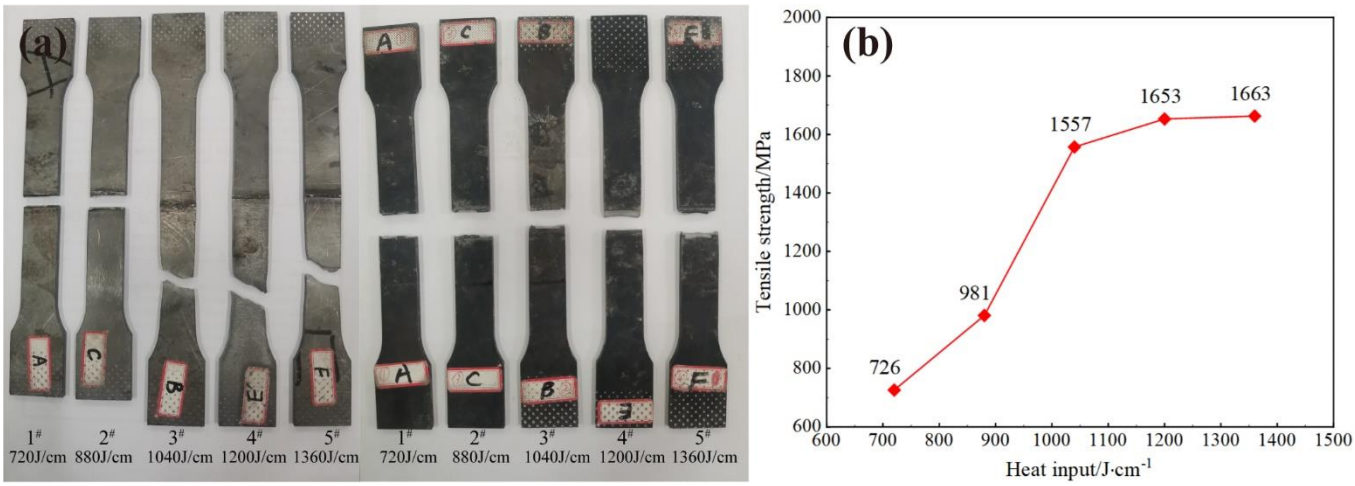

Figure 5. The samples and tensile strength at different heat input (a)samples (b)Tensile strength

Influence of welding speed on macroscopic morphology and strength

The macroscopic morphology of samples at different wire feeding speed at heat input of 1040J/cm is showed in **Fig.6(b)**. At wire feeding speed of 1.4m/min, the upper surface of the joint is sagged seriously because the volume of filling metal is small and the heat input is higher relatively. A large amount of BM was melted and the temperature is extremely high of weld pool, leading to a slow solidification speed. So, the pits on the upper surface are formed under the action of gravity and the force of laser beam on the liquid metal. When the wire feeding speed increased to 1.6m/min, filling metal volume increasing, there are only slight pits on the upper surface at this time. When the wire feeding speed of 1.8m/min, there are basically no pits on the upper surface of the weld and no obvious reinforcement on the lower surface. However, if the wire feed increases continually, a very obvious reinforcement appears on the upper surface of the weld, and the cross section of the weld is showed funnel-shaped at wire feeding speed of 2.0m/min and 2.2m/min. At this moment, the heat input becomes low relative to the increasing wire feeding speed. So, lot of heat melts the welding wire and the heat reflected by wire increase too, a large volume of liquid wire metal rapid solidified on the upper surface of joint and accumulation.

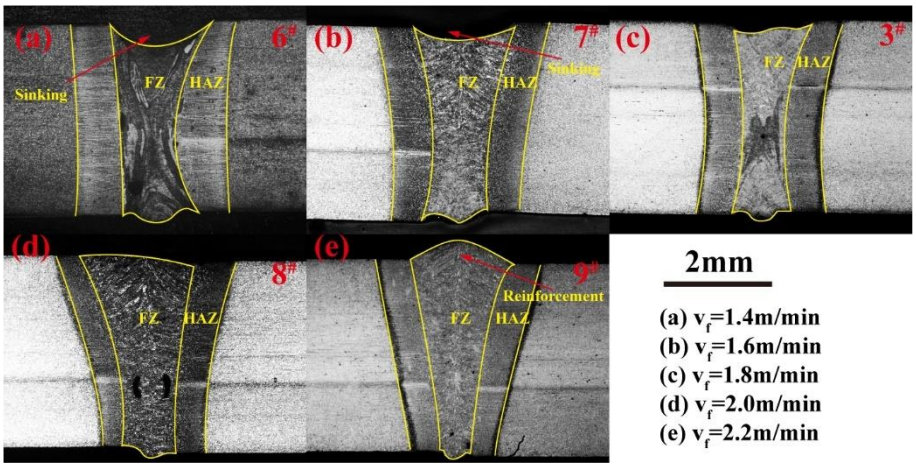

Figure 6. Macro morphologies of joint at different wire feeding speed

The samples and tensile strength at different wire feeding speed when heat input of 1040J/cm are showed in **Fig.7(b)**. When the wire feeding speed of 1.4m/min, the strength

Preprints (www.preprints.org) | NOT PEER-REVIEWED | Posted: 31 May 2021 doi:10.20944/preprints202105.0738.v1

is 574MPa before quenching and 612MPa after quenching because the joint gap is not fully filled. When the wire feeding of 1.6m/min, the filling metal volume increases and the weld strength increases to 1653MPa after quenching, with an excellent strength. When the wire feeding of 1.8m/min, the weld strength was 1557MPa, which was similar with the wire feeding speed of 1.6m/min. But if the wire feeding higher than 1.8m/min, the strength decreases obviously because the base material and the welding wire metal are not fully fused at low heat input. Therefore, it can be found that when the heat input is 1040J/cm, the optimal wire feeding speed is about 1.6-1.8m/min.

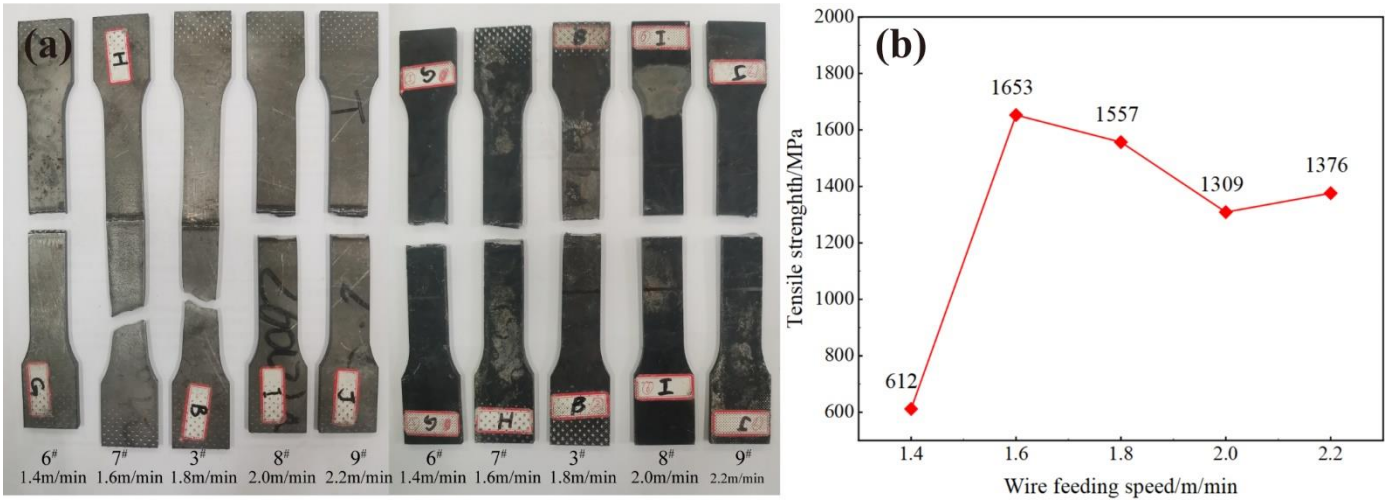

Figure 7. The samples and tensile strength at different wire feeding speed (a) Samples (b) Tensile strength

Microstructure of joints before and after quenching

Microstructure before quenching

The microstructure of the joint before quenching is shown in **Fig.8**. Observing the macroscopic morphology in **Fig.8a**, the joint can be divided obviously into fusion zone (FZ), heat-affected zone (HAZ) and base material (BM). The microstructure of FZ is showed in **Fig.8(b)**, martensite (M) is the main microstructure in this zone due to the rapid cooling speed after laser welding [13]. HAZ can be divided into the coarse-grain zone (CGZ), fine-grain zone (FGZ) and incomplete recrystallization zone (IRZ) according to the degree of transformation [13]. The temperature of CGZ and FGZ had exceeded the Ac_3 line by the function of thermal cycle. The CGZ was close to the FZ and the temperature between the melting point and the superheat temperature. Thus, the austenite grain grown significantly and is transformed into extremely coarse martensite and retained austenite (RA) after rapid cooling as shown in **Fig. 8(c)**. The temperature in FGZ ranged from superheat temperature to Ac_3 line, so the high temperature residence time is shorter and the grain is not obvious growth compared with the CGZ. The martensite FGZ is finer than both the FZ and the CGZ from the **Fig.8(d)**. However, the temperature in this region is between the Ac3 and Ac1, with part of pearlite austenitized and transformed into martensite. The rest of un-austenitized ferrite (F) and pearlite (P) remain its original state as shown in **Fig.8(e)**. **Fig. 8(f)** shows the microstructure of the BM, which didn't get the function of welding thermal cycle and with no microstructure transformation.

Preprints (www.preprints.org) | NOT PEER-REVIEWED | Posted: 31 May 2021 doi:10.20944/preprints202105.0738.v1

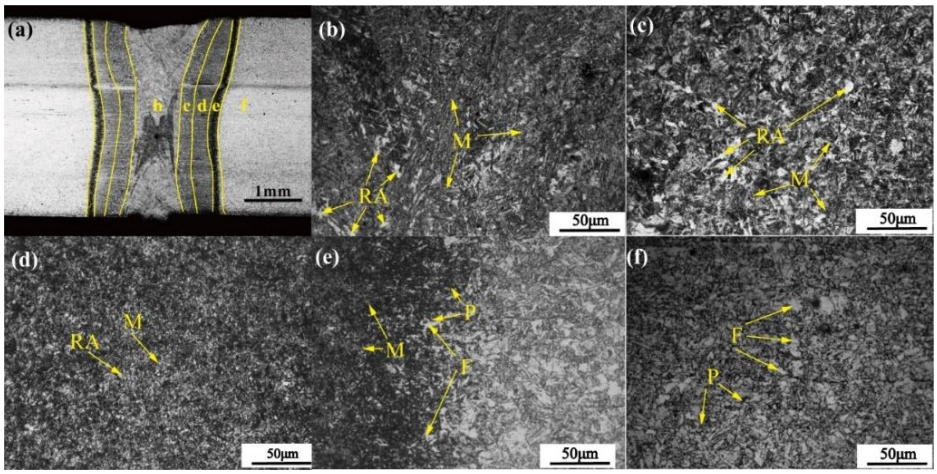

Figure 8. The microstructure of welding joint before quenching (a) Macro morphology (b) FZ (c) CGZ (d) FGZ (e) IRZ (f) BM

Microstructure after quenching

The microstructure of sample quenched in water was showed in **Fig.9**. It is difficult to distinguish the boundary of FZ, HAZ and BM after quenching from the macroscopic morphology shown in **Fig.9(a)**. After quenching, FZ, HAZ, BM have all been transformed into lath martensite and some RA by observing the **Fig.9(b), (c), (d)**. Due to the high heating temperature and fast cooling rate in the quenching process, it could be found that the martensite fraction after quenching was very high, and few fine RA is distributed around the martensite compare with the microstructure before quenching.

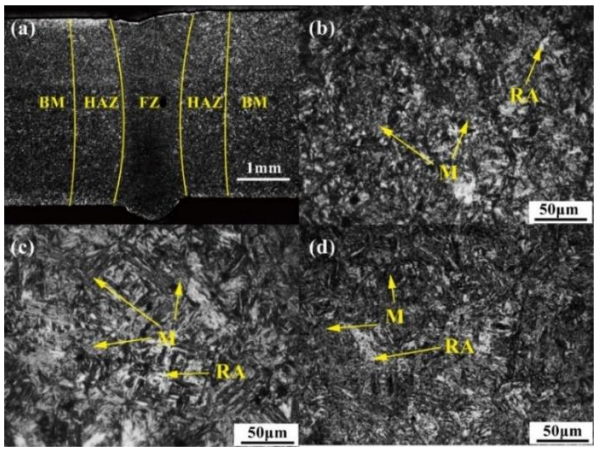

Figure 9. The microstructure of welding joint after quenching (a) Macro morphology (b) FZ zone (c) Original HAZ zone (f) BM

EBSD test

Grain size before and after quenching

The coloured grain of joint before and after quenching is showed in **Fig.10**. The most apparent feature of FZ is that the grain diameter is obviously uneven from the **Fig.10 (a)**. There are coarse grains in the FZ with a large diameter, which is consistent with the coarse martensite observed in the microstructure. Therefore, it also indicates that the overheating in the FZ leads to the serious grain growth. The grain diameter of CGZ and FGZ are relatively uniform, but the grain diameter of CGZ is coarser than that of FGZ, and it could be clearly found that the grain diameter of FGZ is the smallest among all joint. From the **Fig.10 (b)**, after quenching, the original coarse grains in FZ have been completely refined, and the grain diameter among the all joint has been much more uniform than that before quenching. Besides, the grain diameter of CGZ and FGZ is the same after quenching, which can't be clearly distinguished in the **Fig.10 (b)**. However, the grain diameter of the

Preprints (www.preprints.org) | NOT PEER-REVIEWED | Posted: 31 May 2021 doi:10.20944/preprints202105.0738.v1

BM grown up obviously after quenching, which is obviously larger than that of the FZ and HAZ. **Fig.11** shows the statistical results of grain diameter before and after quenching. A very few grains diameter of the joints larger than 15.8μm before and after quenching, and the diameter between 3.1~10.1μm of before quenching, 4.2~10.1μm of after quenching is the main part of the joint grain diameter. In general, the grain diameter is between 3.1 and 10.1μm as the main part in the joint, more than 86.2% and 81.9% before and after quenching respectively. However, the difference is that the FZ have some coarse grain diameter more than 40μm before quenching. But the coarse grain is refined by quenching process, so the maximum grain diameter is less than 27.5μm after quenching, indicating that quenching process have an obviously effect on refining grain size and enhance the strength and toughness of joint.

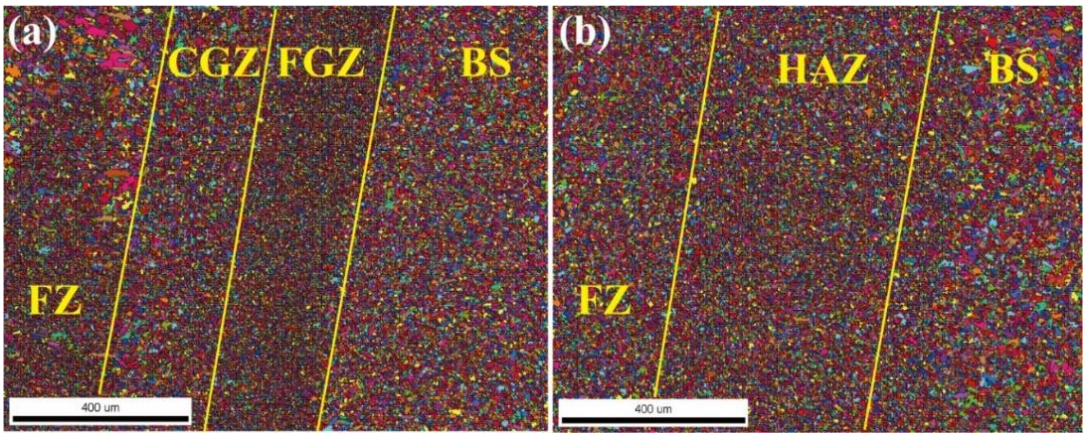

Figure 10. Grain diameter of joint before and after quenching (a) Before quenching; (b) After quenching

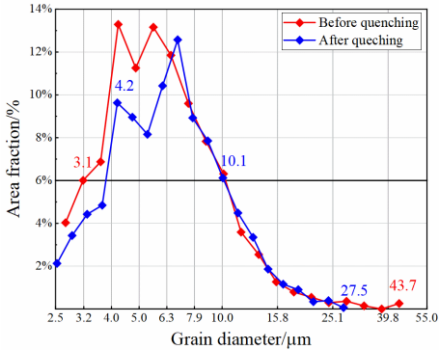

Figure 11. The statistical results of grain diameter

Grain orientation before and after quenching

Fig. 12 shows the grain orientation distribution of the joint before and after quenching. As depicted in **Fig.12(a)**, the BM has obvious orientation of green of {101} before quenching due to rolling process. However, the grain in the FZ is fast cooling from the melting state, showing a random orientation. HAZ has experienced recovery and recrystallization and grain growth by the thermal cycle, showing an no obvious preferred orientation due to thermal cycling compared with BM [17]. **Fig.12(b)** shows the grain orientation of different region of the joint after quenching. It can be found that BM had more orientation of blue {111} and red {001} generated by the quenching process. The whole joint is identified in random orientation after quenching [19-20].

Preprints (www.preprints.org) | NOT PEER-REVIEWED | Posted: 31 May 2021 doi:10.20944/preprints202105.0738.v1

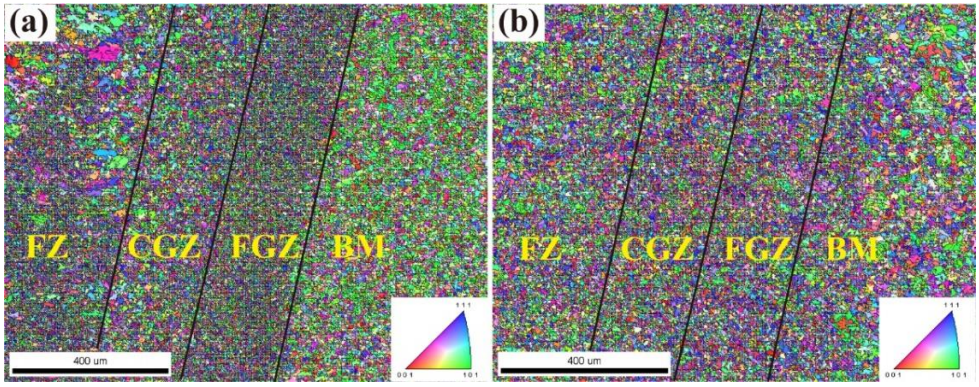

Figure 12. Grain orientation distribution of joints; (a) Before quenching; (b) After quenching

Grain boundary before and after quenching

The grain boundary misorientation and statistical results of the joint before and after quenching is showed in **Fig.13** and **Fig.14**. Before quenching process, the proportion of high-angle misorientation boundary (15°-180°) is 88.5%, while the middle-angle misorientation and low-angle misorientation is 6.8% and 4.7% respectively. Besides, the results shows that more grain boundary orientation is 0°~5° and 25°~60° in the joint. The grain size of FZ region is not uniform, and there are a large number of red boundary (2°-5°) inside the coarse martensite, while more bule boundary (15°~180°) in the FGZ **2**. Compared with FZ and HAZ, BM has most green boundary (5°-15°) as shown in **Fig.13(a)** 20. Showed from the **Fig.13(b)**, more 50°~60° boundary is generated after quenching process but the boundary of 25°~60° is decrease greatly. So, the high-angle misorientation boundary decreases to 86.1% after quenching overall, but the middle-angle misorientation and low-angle misorientation increases to 8.1% and 5.9% respectively. With the grain refinement and homogenization in the FZ and HAZ, the high-angle misorientation boundaries in the FZ and FGZ are reduced and more middle-angle misorientation generated in FZ and FGZ while more low-angle misorientation obviously generated in BM.

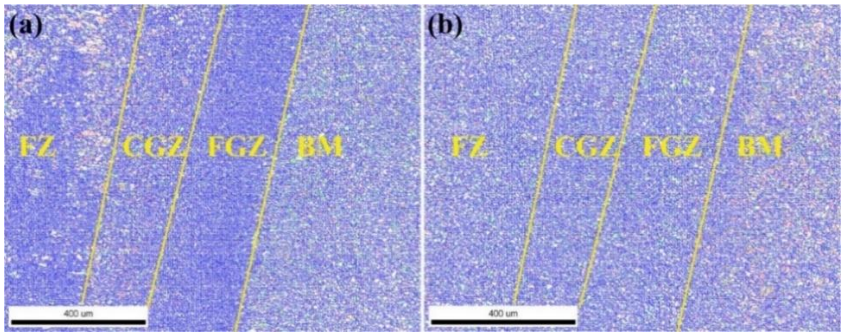

Figure 13. Angle misorientation of joint grain boundary; (a) Before quenching; (b)after quenching

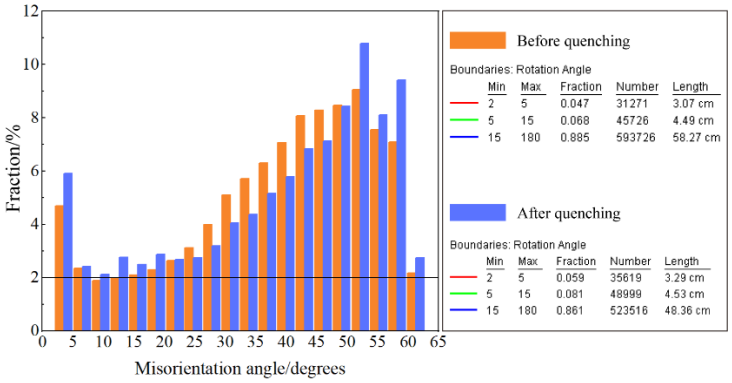

Figure 14. The statistical of misorientation angle before and after quenching

Preprints (www.preprints.org) | NOT PEER-REVIEWED | Posted: 31 May 2021 doi:10.20944/preprints202105.0738.v1

Retained austenite before and after quenching

The retained austenite in joint is analysed by EBSD and its distribution is showed **Fig.15**. From the Figure **15(a)**, the fraction of retained austenite in FZ and FGZ was extremely high and uneven before quenching, which has a great influence on microhardness and strength of FZ. However, the fraction of retained austenite in CGZ is obviously less than that in FZ and FGZ. **Fig.16(b)** shows the distribution of retained austenite in the joint after quenching. With the fraction of 9.1% decreases to 4.4%, less retained austenite exists in the FZ, CGZ and FGZ and distribute evenly. But the fraction of retained austenite in BM increased significantly after the quenching process due to the fast cooling. So, the quenching process distinctly decreases the retained austenite in FZ and HAZ but increases in the BM.

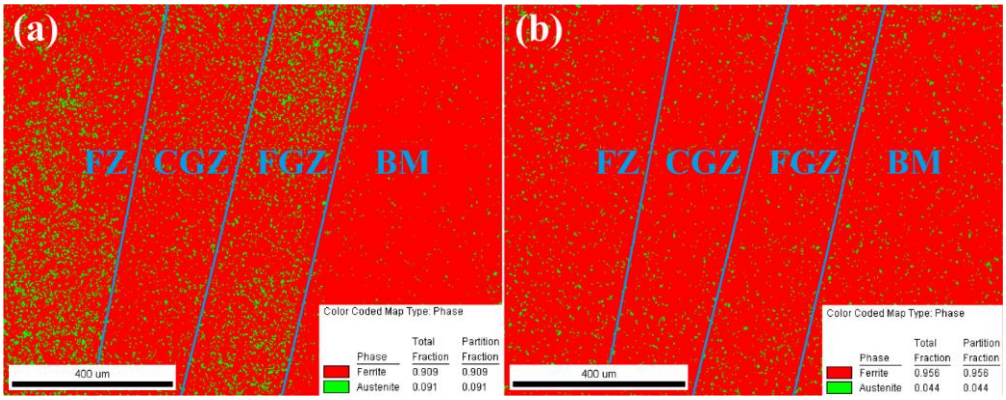

Figure 15. Retained austenite distribution before and after quenching (a) Before quenching; (b) After quenching

Microhardness

The influence heat input on microhardness

Heat input and quenching process have a great influence on the microhardness of joints. **Fig.16** shows the joint microhardness before and after quenching at different heat input. Due to the FZ, CGZ and FGZ contain a lot of martensite, the microhardness is greatly higher than that of BM and IRZ before quenching, which reaches more than 450HV but the BM only 200HV. This is the reason why the strength of joint before quenching is higher than BM. As can be seen from **Fig.16(a)**, with the increase of heat input, the width of FZ and HAZ increases gradually. Besides, the grain growth is obvious as the increase of heat input, resulting the decrease in the microhardness. When the heat input is 720J/cm, 880J/cm and even 1040J/cm, the microhardness of FZ, CGZ and FGZ is more than 500HV, which is obviously higher than that 450HV of 1200J/cm and 1360J/cm.

Fig.16(b) shows the microhardness of the quenched joint at different heat input. The microstructure of FZ, HAZ, BM are all transformed into martensite and few retained austenite and with a uniform grain. So, the microhardness becomes more uniform after quenching, with microstructure of all sample between 450HV-550HV. The microhardness of the BM increases enormously from 200HV to 500HV after quenching, while the FZ, CGZ and FGZ only increase slightly. For the samples of heat input of 880J/cm and 1020J/cm, the microhardness decreases obviously after quenching, but it distributes more evenly on the whole joint and with a better mechanical property. For heat input of 1200J/cm and 1360J/cm, due to the high heat input and grain growth leading to a low microhardness before quenching and the microhardness increased slightly by the grain refined and more martensite generated after quenching. However, from the analysis of all the microhardness before and after quenching, it can be concluded that the quenching process can significantly improve the hardness of BM and IRZ, while homogenize the microhardness and the microstructure of CGZ, FGZ and FZ.

Preprints (www.preprints.org) | NOT PEER-REVIEWED | Posted: 31 May 2021 doi:10.20944/preprints202105.0738.v1

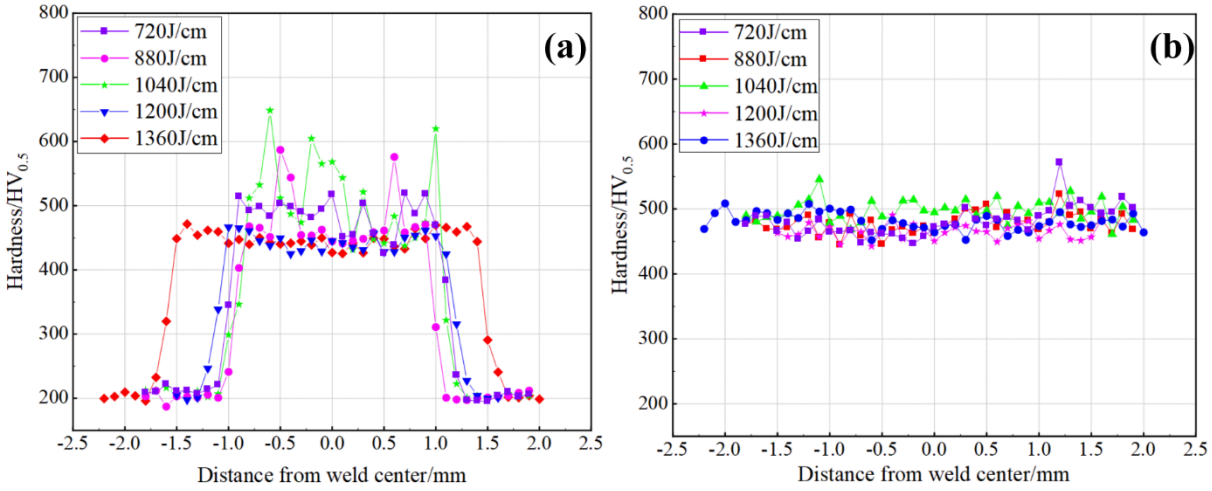

Figure 16. Microhardness of joint at different heat input (a)Before quenching (b)After quenching

The influence of wire feeding speed on microhardness

The microhardness of weld joint at different wire feeding speed when the heat input of 1040J/cm is showed in **Fig.17**. It can be observed from **Fig.17(a)** clearly that the microhardness of FZ is about 375HV at wire feed speed of 1.4m/min and 1.6m/min before quenching. It may because the low wire feeding speed and the high heat input, leading to the high temperature of FZ and the grain growth. So, when the wire feeding speed increase to 1.8m/min, the microhardness of FZ increase suddenly due to the volume of wire metal increase. Then, if the wire feeding of 2.0m/min and 2.2m/min, the microhardness of FZ and HAZ keeps on 450HV to 500HV. So, it can be concluded that with the wire feeding speed increase, the increase of wire metal volume will increase the microhardness of FZ in some extent.

Fig.17(b) shows the microhardness of joint at different wire feeding speed after quenching. With the quenching process, the whole joint microhardness is between 450-550HV, and it is similar with the **Fig16(b)**. So, by analysing the microhardness, the heat input and wire feeding speed only affect the microhardness before quenching of joint, and have less effect on the joint microhardness after quenching.

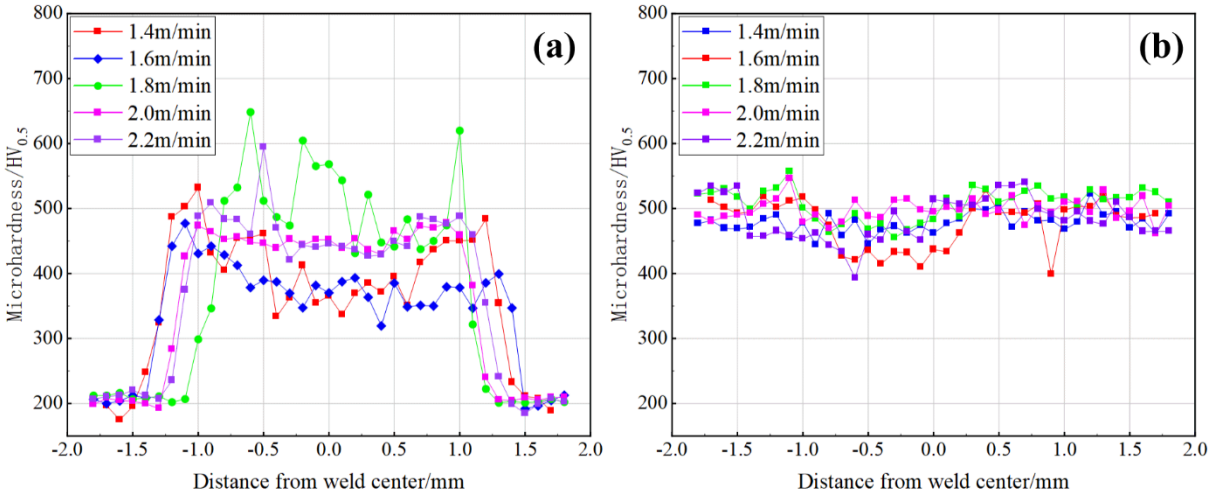

Figure 17. The microhardness of joint at different wire feeding speed (a)Before quenching (b)After quenching

Fracture morphology

Fig. 18 shows the fracture morphology of the joint and BM before quenching. A large number of dimples and section of river patterns can be observed on the fracture morphology. So, the ductile fracture indicates that the weld joint before quenching has a good

Preprints (www.preprints.org) | NOT PEER-REVIEWED | Posted: 31 May 2021 doi:10.20944/preprints202105.0738.v1

plasticity [19]. However, some river patterns and many voids are also observed in the dimples, mainly due to the high martensite strength and poor ductility after quenching, and a large number of secondary cracks and dissociation platform occur during the tensile process [21]. The dimples in **Fig.18(b)** are cup-shaped dimples with large depth mixed with a large number of voids. The dimples in **Fig.18(c)** are is axial dimples with small depth and nearly round shape, and a large number of second-phase particles are observed at the bottom of the dimples. **Fig. 18(d)** shows the tensile fracture of BM before quenching. The dimples of BM are denser and more small dimples with less secondary cracks. The surface of the fracture is more uneven, resulting in greater plastic deformation during stretching.

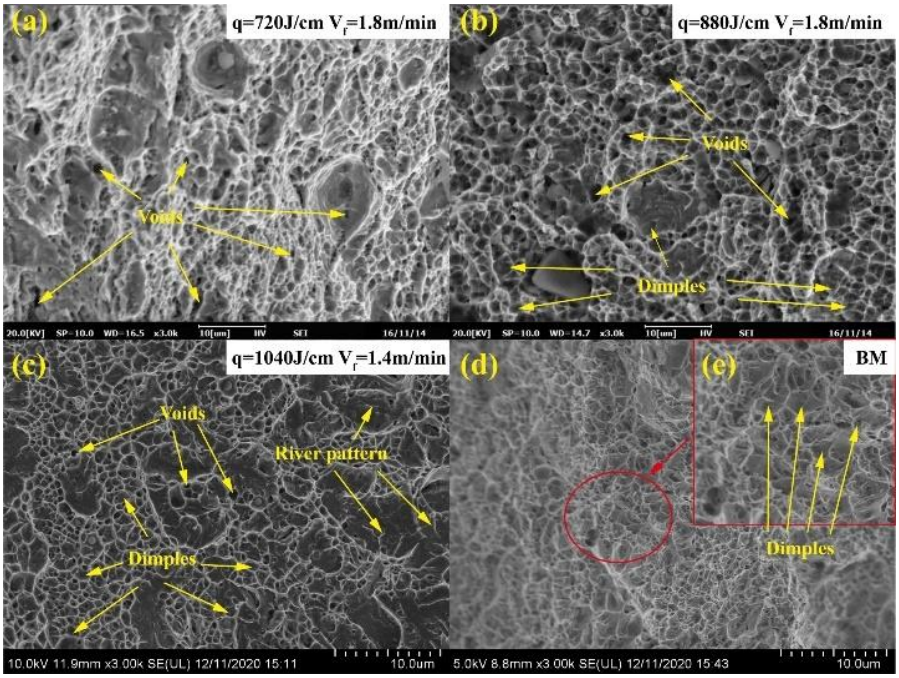

Figure 18. Tensile fracture morphology of different parameters before quenching

Fig. 19 shows the fracture morphology of joint and BM after quenching. The microstructure of joint combine with high strength and brittleness martensite. So, the cleavage facet, large number of dissociation river pattern and a small number of shallow dimples is showed in the fracture morphology after quenching. Besides, the fracture morphology is flat and with smaller plastic deformation before fracture, indicating a brittle fracture of the joint after quenching. Especially from the **Fig.19(a)** and **(b)**, the fracture almost constitutes of cleavage step and river pattern. **Fig. 19(d)** shows the fracture morphology of BM after quenching. The fracture morphology of BM fracture is flat and a large number of shallow dimples distributed. But compare with the BM before quenching, the BM has less plasticity after quenching process with elongation of about 6%.

Preprints (www.preprints.org) | NOT PEER-REVIEWED | Posted: 31 May 2021 doi:10.20944/preprints202105.0738.v1

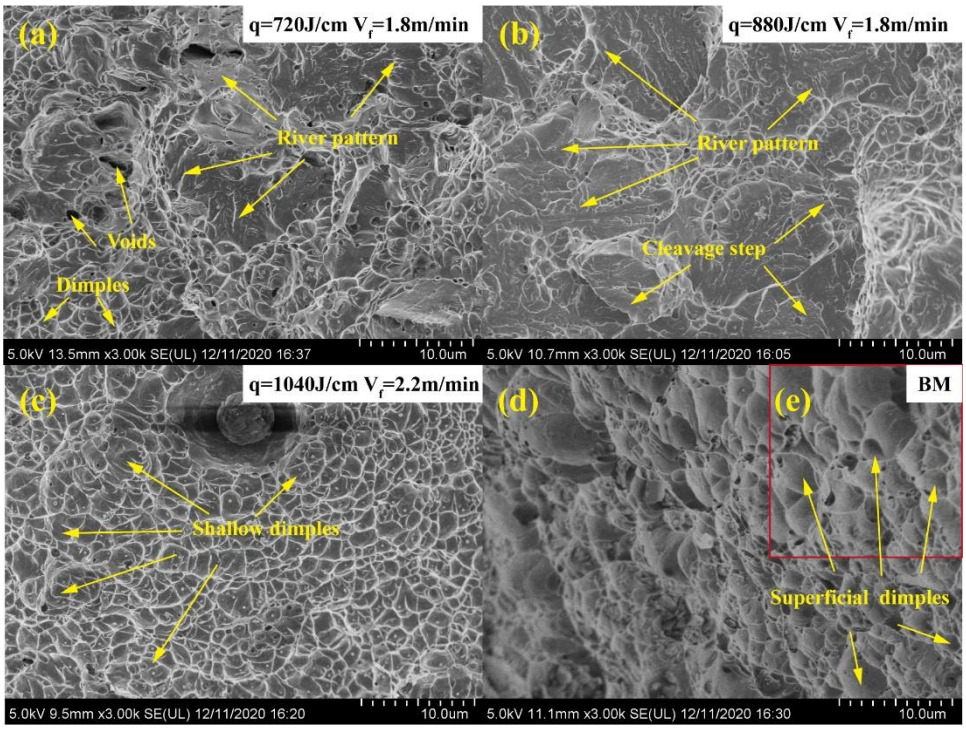

Figure 19. Tensile fracture morphology of different parameter after quenching

4. Conclusions

The 3.5mm thickness BR1500HS boron steel was weld by fiber wire-filling laser welding with gap of 0.5mm, with laser power of 1800w to 3400w at wire feeding speed of 1.8m/min and wire feeding speed of 1.4m/min to 2.2m/min at laser power of 2600w, and welding speed keeps of 1.5m/min unchanged for all samples. The experiment result analysis can lead to the following conclusions:

The macroscopic morphology of FZ is funnelform at heat input less than 1040J/cm and becomes hyperbolic curve shape if heat input more than 1040J/cm. The strength after quenching is more than 1557Mpa at heat input more than 1040J/cm.

The macroscopic morphology is hyperbolic curve shape at wire feeding speed less than 1.8m/min and becomes funnelform when wire feeding speed more than 1.8m/min. The joint has an excellent strength at wire feeding speed between 1.6m/min~1.8m/min.

The microstructure of FZ, CGZ, FGZ before quenching are martensite and retained austenite. Besides, the FZ and FGZ have more retained austenite than CGZ. After quenching, the microstructure of FZ, HAZ and BM is almost martensite and few retained austenite. The retained austenite in FZ and HAZ decreased clearly and distributed uniformed, while the retained austenite in the BM have increased due to the quenching process.

Before quenching, FZ have an uneven distribution of grain and some grain diameter have larger than 40μm. The grain of FGZ is the smallest in the whole zone and the CGZ have the similar grain diameter with BM. After quenching, the grain diameter of FZ, HAZ and BM is more even and large grains in the FZ have been refined. Besides, the phenomenon of grain growth in BM have been observed. The grain diameter is between 3.1 and 10.1μm as the main part in the joint, more than 86.2% and 81.9% before and after quenching respectively.

Before quenching, the microhardness of FZ and HAZ decreased from 500HV to 450HV with the increase of heat input. But as the wire feeding speed increases, the microhardness of FZ and HAZ increased from 450HV to 500HV. After quenching, the microstructure of all samples keeps at 450HV~550HV, and the microstructure of FZ, HAZ and BM is no difference. So, heat input and wire feeding speed have less effect on the microhardness of joint after quenching.

A large amount of dimple and little river pattern int the fracture morphology of joint before quenching indicates a well plasticity. But after quenching, a large amount of river pattern and cleavage facets are observed in fracture morphology due to the joint combine with high strength and brittleness martensite.

Funding: This research and the APC was funded by Suizhou-WUT Industry Research Institute grant number suikefa[2019]9.

Data Availability Statement: The date presented in this study are available in this article.

Conflicts of Interest: The authors declare no conflict of interest.

References

1. Gu X, Wu S, Duan Z, et al. Effect of welding parameters on weld formation quality and tensile-shear property of laser welded SUS301L stainless steel lap filet weld. *J Mater Res Technol* 2020, 9, 4840-4854.
2. Mao G, Cayron C, Cao R, et al. The relationship between low-temperature toughness and secondary crack in low-carbon bainitic weld metals. *Mater Charact* 2018, 145, 516-526.
3. Prasad H S, Frostevarg J, Kaplan A F H. The stability of laser welding with an off-axis wire feed. *J Mater Process Tech* 2019, 264, 84-90.
4. Bunaziv I, Wenner S, Ren X, et al. Filler metal distribution and processing stability in laser-arc hybrid welding of thick HSLA steel. *J Manuf Process* 2020, 54, 228-239.
5. Zhang S, Sun J, Zhu M, et al. Fiber laser welding of HSLA steel by autogenous laser welding and autogenous laser welding with cold wire methods. *J Mater Process Tech* 2020, 275,116353.
6. Wang H, Wang Y, Li X, et al. Influence of Assembly Gap Size on the Structure and Properties of SUS301L Stainless Steel Laser Welded Lap Joint. *Materials* 2021, 14, 996.
7. Acherjee B. Hybrid laser arc welding: State-of-art review. *Opt Laser Technol* 2018, 99,60-71.
8. Pu J, Zhao Y, Jiang Y, et al. Influence of wire feeding speed on the melting behavior and formation of narrow-gap joint by laser welding with filler wire. *J Laser Appl* 2020, 32, 032007.
9. Zhao Y, Ma S, Huang J, et al. Narrow-gap laser welding using filler wire of thick steel plates. *Int J Adv Manuf Tech* 2017, 93, 2955-2962.
10. Ahn J, Chen L, He E, et al. Effect of filler metal feed rate and composition on microstructure and mechanical properties of fibre laser welded AA 2024-T3. *J Manuf Process* 2017, 25, 26-36.
11. Yang M, Lu J, Chen J, et al. Effect of welding speed on microstructure and corrosion resistance of Al–Li alloy weld joint. *Mater Corros* 2020, 71, 300-308.
12. Lee H W, Yoo K J, Tran M T, et al. Effect of Quenching Tempering-Post Weld Heat Treatment on the Microstructure and Mechanical Properties of Laser-Arc Hybrid-Welded Boron Steel. *Materials* 2019, 12, 2862.
13. Li M, Yao D, Guan Y, et al. Effect of Welding Speed and Post Quenching on the Microstructure and Mechanical Properties of Laser-Welded B1500HS Joints *Materials* 2020, 13, 4645.
14. Das C R, Albert S K, Bhaduri A K, et al. Effect of boron addition and initial heat-treatment temperature on microstructure and mechanical properties of modified 9Cr-1Mo steels under different heat-treatment conditions. *Metall Mater Trans A* 2013, 44, 2171-2186.
15. Lin W, Li F, Hua X, et al. Effect of filler wire on laser welded blanks of Al-Si-coated 22MnB5 steel. *J Mater Process Tech* 2018, 259, 195-205.
16. Saha D C, Biro E, Gerlich A P, et al. Fiber laser welding of AlSi coated press hardened steel. *Weld J* 2016, 95, 147-156.
17. Zhao H, Huang R, Sun Y, et al. Microstructure and mechanical properties of fiber laser welded QP980/press-hardened 22MnB5 steel joint. *J Mater Res Technol* 2020, 9, 10079-10090.
18. Chen L, Nie P, Qu Z, et al. Influence of heat input on the changes in the microstructure and fracture behavior of laser welded 800MPa grade high-strength low-alloy steel. *J Manuf Process* 2020, 50, 132-141.
19. Fang N, Guo E, Huang R, et al. Effect of welding heat input on microstructure and properties of TC4 titanium alloy ultra-narrow gap welded joint by laser welding with filler wire. *Mater Res Express* 2021, 8, 016511.
20. Gu X, Cui Z, Gu X, et al. Wire-Feeding Laser Welding of Copper/Stainless Steel Using Different Filler Metals. *Materials* 2021, 14, 2122.
21. Mihaliková M, Zgodavová K, Bober P, et al. The Performance of CR180IF and DP600 Laser Welded Steel Sheets under Different Strain Rates *Materials* 2021, 14, 1553.